Design and Development of Potential Tissue Engineering Scaffolds from Structurally Different Longitudinal Parts of a Bovine-Femur

Sumit **PRAMANIK**[1,*], Belinda **PINGGUAN-MURPHY**[1], Jongman **CHO**[2] & Noor Azuan **ABU OSMAN**[1]

[1]Centre for Applied Biomechanics, Department of Biomedical Engineering, Faculty of Engineering, University of Malaya, Kuala Lumpur 50603, Malaysia

[2]Department of Biomedical Engineering, Inje University, Gimhae, 621-749, Republic of Korea

*Correspondence to: S. P. (prsumit@gmail.com; prsumit@um.edu.my)

Supplementary Information

Appendix A

Crystallite size (t) is evaluated following Debye Scherrer formula in Eq. (S1).

$$t = \frac{\kappa\lambda}{\Delta\theta_{FWHM}\cos(\theta_B)} \qquad \text{(S1)}$$

where, κ is a constant (e.g., 0.9), $\Delta\theta_{FWHM}$ (in radian) is full width at half maxima (FWHM) at $2\theta_B$, and θ_B (in degree) is Bragg's angle.

The crystallite size and crystallinity of all the FBCBs computed from XRD patterns are illustrated in Table S1. Since the trends in crystallite size and crystallinity from distal and middle parts are quite similar to the proximal part, XRD pattern of all the specimens, including *as-received* and heat-treated specimens, only from the proximal part is depicted in Figure S1. The crystal formation starts above at or above 750°C as the crystalline peaks of hydroxyapatite (HA) become sharp.

Table S1. Crystallite size and crystallinity of all the FBCBs evaluated from XRD patterns.

Heat treatment temperature (°C)	Crystallite size[#] (nm)			Crystallinity[*] (%)		
	Distal	Middle	Proximal	Distal	Middle	Proximal
Untreated	32.42	30.52	28.96	30.73	29.08	27.02
120	25.80	25.18	24.68	43.04	35.25	31.15
350	20.45	16.92	28.89	39.65	31.41	30.20
500	29.49	32.34	27.37	67.76	56.71	54.53
750	73.11	75.12	66.47	94.14	93.53	89.93
900	79.88	86.69	82.46	95.29	94.36	90.73
1000	86.53	96.48	96.69	91.02	90.63	87.15

[#]Average crystallite size±20%Deviation; [*]Average crystallinity±2%Deviation.

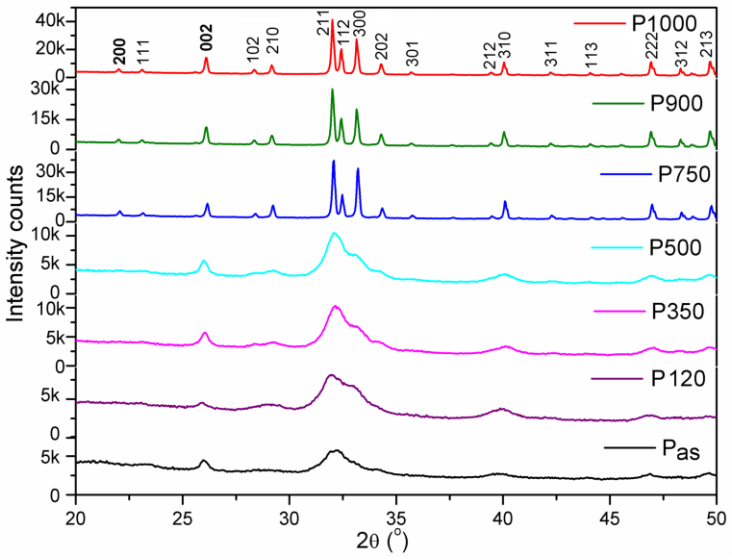

Figure S1. XRD patterns of FBCBs from proximal end, *as-received* (P_{as} – Black) and after heat-treatments at 120°C (P120 – Purple), 350°C (P350 – Magenta), 500°C (P500 – Cyan), 750°C (P750 – Blue), 900°C (P900 – Green), and 1000°C (P1000 – Red) temperatures. Hydroxyapatite (HA) crystal formation starts at or above 750°C.

Appendix B

An inside morphology of a cross-sectional face perpendicular to the femoral axis for a specimen, D900, and its outer face parallel to the bone length, were captured for a sample under field emission scanning electron microscope (FESEM), is depicted in Figure S2. The magnified images indicate that the inner morphologies of both the cross-sectional face and parallel face with respect to bone axis in a specific sample such as D900 are same. Particle and porous morphologies of inside the materials are almost identical for both cross-sectional and outer faces of the material.

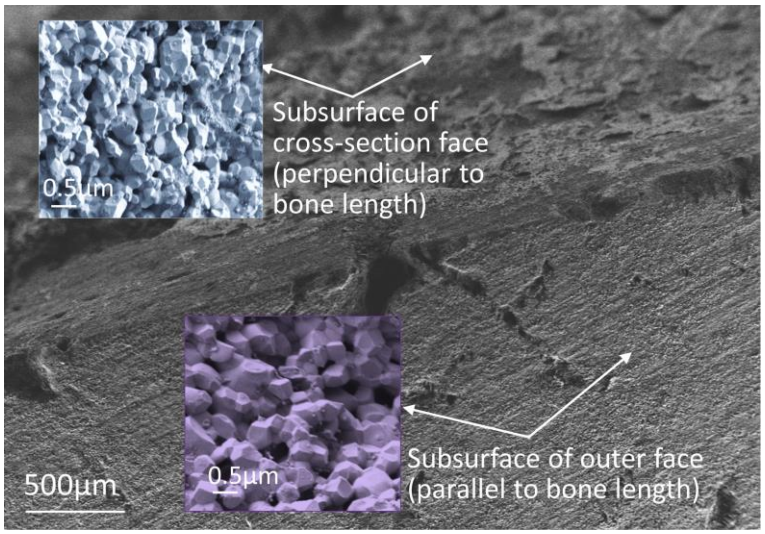

Figure S2. FESEM images at inside morphology of cross-section and outer face with respect to bone axis in D900 sample. Inset images shows that the magnified morphology, including interconnected uniform porous scaffold structure, inside the cross-section and outer faces is almost same.

Table S2. Atomic percentages of carbon and oxygen, and Ca/P molar ratio at proximal end of FBCBs from EDAX data.

Temperature (°C)	C±SD (At%)	O±SD (At%)	Ca/P±SD (At% ratio)
P_{as}	66.8±8.0	30.1±0.3	0.619±0.10
P120	40.8±7.5	36.9±7.9	1.197±0.03
P350	13.8±2.0	56.8±1.5	1.463±0.10
P500	11.4±0.4	55.1±1.2	1.508±0.06
P750	5.9±0.8	55.2±4.1	1.498±0.06
P900	4.5±1.3	57.4±1.1	1.617±0.10
P1000	3.8±0.4	57.8±0.9	1.708±0.04

SD: Standard deviation.

Appendix C

Table S3. Bulk density and open porosity of *as-received* and heat-treated bones.

Sample	Heat treatment (°C)	Density±SD (g/cc)	Open Porosity±SD (%)	Close Porosity±SD (%)
D_{as}	Untreated	1.98±0.01	2.28±0.77	9.83±0.42
M_{as}	-do-	1.70±0.18	17.77±6.03	22.74±8.35
P_{as}	-do-	1.66±0.03	12.52±5.29	24.73±1.20
D120	120	2.02±0.05	2.31±0.05	8.36±2.40
M120	-do-	1.91±0.06	15.12±8.74	13.32±2.61
P120	-do-	1.80±0.07	29.77±6.86	18.4±3.03
D350	350	1.51±0.06	15.72±2.92	52.32±1.92
M350	-do-	1.49±0.03	30.64±6.67	52.83±0.84
P350	-do-	1.44±0.06	42.52±8.80	54.49±2.01
D500	500	1.20±0.14	33.02±0.45	62.00±4.37
M500	-do-	1.37±0.15	36.05±3.60	56.75±4.66
P500	-do-	1.47±0.14	45.63±6.16	53.52±4.33
D750	750	1.50±0.07	2.04±0.88	52.50±0.08
M750	-do-	1.49±0.07	14.12±4.88	52.72±2.28
P750	-do-	1.48±0.03	15.59±3.75	53. 07±1.03
D900	900	1.35±0.03	10.28±1.45	57.17±0.93
M900	-do-	1.33±0.04	15.08±2.298	58.01±1.23
P900	-do-	1.30±0.06	18.68±3.82	58.86±1.78
D1000	1000	1.62±0.02	4.90±0.01	50.66±2.24
M1000	-do-	1.61±0.086	9.23±1.78	50.86±2.39
P1000	-do-	1.60±0.06	10.38±1.62	50.54±2.96

Appendix D

Table S4. Bone mineral properties of FBCBs heat-treated at 120˚C obtained from microCT.

Properties	D120	M120	P120
Porosity, Por [%]	3.15	5.41	15.50
Bone mineral volume, BV [mm^3]	6.2615	2.9819	3.2854
Bone mineral surface, BS [mm^2]	6.0076	3.2679	9.0281
Total volume, TV [mm^3]	6.4655	3.1524	3.8881
BV/TV [%]	96.85	94.59	84.50
BS/BV [mm^{-1}]	0.9594	1.0959	2.7480